NATIONAL ADVISORY COMMITTEE FOR AERONAUTICS

TECHNICAL NOTE 2392

CHARTS GIVING CRITICAL COMPRESSIVE STRESS OF CONTINUOUS FLAT SHEET DIVIDED INTO PARALLELOGRAM-SHAPED PANELS

By Roger A. Anderson

Langley Aeronautical Laboratory
Langley Field, Va.

Washington
July 1951

NATIONAL ADVISORY COMMITTEE FOR AERONAUTICS

TECHNICAL NOTE 2392

CHARTS GIVING CRITICAL COMPRESSIVE STRESS OF CONTINUOUS FLAT SHEET DIVIDED INTO PARALLELOGRAM-SHAPED PANELS

By Roger A. Anderson

SUMMARY

Charts giving the compressive-buckling-stress coefficients for sheet panels of a shape occurring in swept-wing plan forms are presented. The panels are assumed to be a part of a continuous flat sheet divided by nondeflecting supports into parallelogram-shaped areas. The stability analysis was performed by the energy method and the results show that, over a wide range of panel aspect ratio, such panels are decidedly more stable than equivalent rectangular panels of the same area.

INTRODUCTION

A highly desirable characteristic for high-speed flight is to have aircraft outer surfaces that remain free of buckles or waves under all normal flight conditions. Whether these surfaces remain smooth under flight loads is determined by the skin thickness and the arrangement and rigidity of the internal supporting structure to which the skin is attached. In the past, the supporting structure generally divided the outer skin into an array of approximately rectangular panels, but present-day swept- and delta-wing plan forms call attention to the fact that skin panels of other shapes such as parallelograms may occur.

The present paper considers the stability under compressive stress of continuous flat sheet divided by nondeflecting supports into an array of parallelogram-shaped panels. Wide ranges of panel skewness and aspect ratio were investigated, and two orientations of the parallelogram-shaped panels with respect to the direction of the applied stress were considered. The results of the analysis are presented in the form of charts of theoretical buckling-stress coefficients as a function of panel skewness and aspect ratio.

SYMBOLS

x,y	mutually perpendicular directions, rectangular coordinate system
x'	direction parallel to x-direction, skew coordinate system
y'	arbitrary direction, skew coordinate system
ϕ	skew angle between y- and y'-directions, measured positive clockwise from y-direction, degrees
a	panel dimension in x- or x'-direction
b	panel dimension in y-direction
b'	panel dimension in y'-direction
β	panel aspect ratio (a/b)
t	plate thickness
w	deflection normal to plane of plate
D	plate flexural stiffness
μ	Poisson's ratio for plate material
σ	general notation for stress
σ_x	stress acting in x-direction, compression positive
σ_y	stress acting in y-direction, compression positive
k,k_x,k_y	critical-stress coefficients $\left(k = \frac{\sigma t b^2}{\pi^2 D};\quad k_x = \frac{\sigma_x t b^2}{\pi^2 D};\quad k_y = \frac{\sigma_y t b^2}{\pi^2 D}\right)$
V	internal bending energy
T	external work of applied stress

N,M,p,q,j,m,n integers

a_{mn},b_{mn} Fourier coefficients

DESCRIPTION OF PROBLEM

An idealized arrangement of the supporting structure possible for swept and delta wings is shown in figure 1, wherein a part of a continuous flat sheet infinite in length and width is shown divided by nondeflecting supports into an array of parallelogram-shaped panels, of which rectangular panels are a special case. For the case of rectangular panels the assumption is usually made that, if the supporting members are torsionally weak, the plate bending moments arising during plate buckling under edge compression stress are negligible at the panel boundaries and each panel therefore may be treated as an isolated rectangular plate with simply supported edges. Stability data for such panels are available in standard textbooks, such as reference 1.

When a simply supported rectangular plate in compression is skewed into the shape of a parallelogram, a certain increase in stability due to the shape change is achieved, as shown by the numerical examples in reference 2. A further increase in stability is possible when the skewed panels are part of a continuous sheet because of the restraint the adjacent sheet panels impose on each other during the formation of a continuous buckle pattern. The effect of this type of restraint is illustrated in reference 3 for the case of continuous sheet divided into square panels subject to shear stress. Restraint due to sheet continuity would be present in the case of parallelogram-shaped panels regardless of whether the loading is edge compression or shear.

Two orientations of the parallelogram-shaped panels with respect to the principal direction of the compressive stress due to wing bending are considered in the present paper. The two loading conditions are: stress acting parallel to a set of panel sides and stress acting perpendicular to a set of panel sides. Both loading conditions are shown in figure 1.

In the analysis the assumption is made that the supporting members are rigid enough to prevent deflection of the sheet at the panel boundaries but offer no restraint to rotation. A quantitative analysis of the stiffnesses required of supporting members (ribs, stiffeners, shear webs, etc.) to prevent deflection around the edges of parallelogram-shaped sheet panels is beyond the scope of this paper, but indications are that they would be somewhat higher than the stiffness required to support equivalent rectangular sheet panels.

In order to establish a stability criterion for the configuration analyzed, the energy method of analysis is used, and an approximation is made for the deflection of the plate expressed in skew coordinates (see appendix A). The deflection function used leads to the exact solution of the differential equation of equilibrium of the plate loaded in compression for the special case of rectangular panels and also for the special case of equal-sided panels of arbitrary skewness subjected to compressive loading perpendicular to one set of sides. The accuracy of the rest of the data is indicated, where feasible, by comparison with the results of more accurate energy solutions, which are given in appendix B.

RESULTS AND DISCUSSION

The critical compressive stress for parallelogram-shaped plates may be given by the formula used for rectangular plates

$$\sigma t = k \frac{\pi^2 D}{b^2}$$

where the dimension b is the perpendicular distance between the supports alined in the x-direction, as in figure 1. The critical-stress coefficient k depends on the panel aspect ratio β (defined as a/b), the direction of the applied compressive stress, and the magnitude of the skew angle ϕ.

For loading in the x-direction (stress acting parallel to a set of sides), the chart for k_x is given in figure 2. Note should be taken that, for a given value of β, the buckling coefficients indicated for each curve are associated with panels of equal area. In order to facilitate association of the curves of figure 2 with the geometry of the panels, figure 3 has been prepared. In this figure, sketches of the panels of aspect ratios of 1, 2, and 3 are presented along with four of the curves of figure 2. In each sketch the mode of buckling for the panel is indicated. Figures 2 and 3 indicate that the stability of the skewed panels is definitely increased relative to equivalent rectangular panels of the same area over a wide range of panel aspect ratio. This increase in stability is due partly to the change in panel shape but is caused mainly by the restraint imposed on the mode of buckling due to the presence of adjacent skewed panels. At aspect ratios of 4.5 and greater, this restraint has largely disappeared and the coefficients approach the value 4.

The curves presented in figures 2 and 3 were derived by the energy method of analysis with the use of an assumed deflection function capable

of giving an idealized representation of the panel buckling modes. The buckling coefficients thus obtained represent upper limits to the true coefficients. In order to evaluate the unconservativeness of the curves presented in figures 2 and 3, check calculations were made by energy solutions of greater accuracy. The results of these calculations, which are believed to be less than 1 percent unconservative, are indicated by the circles near the curves in figures 2 and 3. Because of the complexity of the buckle patterns, check calculations over the entire range of aspect ratio were not feasible to make, but it seems reasonable that the remaining parts of the curves would show about the same degree of unconservativeness as in the regions where check calculations were made. The numerical values of the circles in figures 2 and 3 are listed in table 1.

For loading in the y-direction (stress acting perpendicular to a set of sides), the chart for k_y is presented in figure 4. These curves show that a single buckle pattern (characterized by an alternate in and out buckling from panel to panel) exists throughout the range of aspect ratio investigated except for the expected change in mode at aspect ratio $1/\sqrt{2}$ for the $\phi = 0^\circ$ case. Again, the effect of continuity between panels on the buckling coefficient has largely disappeared at aspect ratios of 4.5 and greater. The squares on these curves indicate the points at which the derived curves pass through the exact value for the buckling coefficient, and the results of energy solutions of high accuracy indicated by the circles are in excellent agreement with the remaining parts of the derived curves. (See table 1 for numerical values.)

Under the simultaneous action of compressive stresses in the x- and y-directions, the critical-stress combinations for a given panel can be shown by means of an interaction curve. A family of such curves is presented in figure 5 for an array of equal-sided panels for various angles of skewness of the panels. It is rather interesting that for equal-sided panels the stability criterion for a σ_y type of stress acting alone is independent of ϕ and gives a constant value of 4 (exact) for the buckling coefficient.

The interaction curves for $\phi = 45^\circ$ and 60° in figure 5(a) have been adjusted in the regions where the more accurate energy solutions showed that the energy solution using an idealized representation of the buckling modes was unconservative. The relation between the more accurate check calculations and the approximate solution is shown in figure 5(b). The discontinuities in slope of the curves for $\phi = 45^\circ$ and 60° in this figure indicate that several changes in buckling mode take place in passing from a σ_y type of stress to a σ_x type of stress. The smooth curves in figure 5(a), however, were obtained by simply fairing a curve through the check points of figure 5(b). The numerical values of the check points are included in table 1.

CONCLUDING REMARKS

The charts presented show that the stability of flat continuous sheet divided by supporting members into skewed panels is definitely increased in relation to the stability of equivalent rectangular panels of equal area over a wide range of panel aspect ratio. This increase in stability may be attributed partly to the nonrectangular shape of the panels but is caused mainly by the restraint imposed on the mode of buckling due to the presence of adjacent skewed panels.

Langley Aeronautical Laboratory
National Advisory Committee for Aeronautics
Langley Field, Va., April 5, 1951

APPENDIX A

APPROXIMATE SOLUTION FOR CRITICAL COMPRESSIVE STRESS OF FLAT PLATE CONTINUOUS OVER SKEWED SUPPORTS

Consideration of a flat plate supported and loaded as shown in figure 1 reveals that, for many combinations of plate aspect ratio and skew angle, a rather complex deflection pattern might be expected when buckling occurs. The associated plate differential equation of equilibrium written in skew coordinates (x',y') is

$$\frac{\partial^4 w}{\partial x'^4} + 2(1 + 2\sin^2\phi)\frac{\partial^4 w}{\partial x'^2 \partial y'^2} + \frac{\partial^4 w}{\partial y'^4} - 4\sin\phi\left(\frac{\partial^4 w}{\partial x'^3 \partial y'} + \frac{\partial^4 w}{\partial x' \partial y'^3}\right) =$$

$$-\frac{\sigma_x t}{D}\frac{\partial^2 w}{\partial x'^2}\cos^4\phi - \frac{\sigma_y t}{D}\cos^2\phi\left(\frac{\partial^2 w}{\partial x'^2}\sin^2\phi - 2\frac{\partial^2 w}{\partial x' \partial y'}\sin\phi + \frac{\partial^2 w}{\partial y'^2}\right)$$

This equation further indicates that for arbitrary panel dimensions an exact solution for the deflection w is not likely to be found. It is interesting, however, that for the particular case of equal-sided skew panels under compression stress acting perpendicular to one set of sides, the familiar deflection function

$$w = \sin\frac{\pi x'}{a}\sin\frac{\pi y'}{a}$$

written in skew coordinates is the exact solution to the differential equation. The resulting stability criterion is independent of the skew angle ϕ and the buckling-stress coefficient k_y is equal to 4, or

$$\sigma_y t = \frac{4\pi^2 D}{b^2}$$

The points where this solution applies have been noted on the curves of figure 4. In order to calculate the buckling-stress coefficients for other panel dimensions, the energy method can be used with an assumed expression for the plate deflection.

Choice of deflection function.- The foregoing example indicates that, for skewed panels compressed in a direction perpendicular to one set of sides (y-direction in fig. 1), a single skewed sinusoidal wave in each panel is a good assumption for a deflection function for panels of equal or nearly equal sides. This assumption is also made for panels of larger aspect ratio. For compression loading parallel to one set of sides (x-direction in fig. 1), however, it is evident that for most of the range of aspect ratio, several buckles will form in each panel. Each panel therefore would contain contours of zero deflection, or nodal lines, between buckles. Since continuity of deflection and slope must be preserved at the panel boundaries, the nodal lines must run continuously across panel boundaries. For example, skewed panels of large aspect ratio under stress in the x-direction would buckle in such a manner that a system of rather uniformly spaced nodal lines would develop between buckles and would run continuously in the general direction of the y-coordinate. This characteristic behavior, idealized in the following sketch,

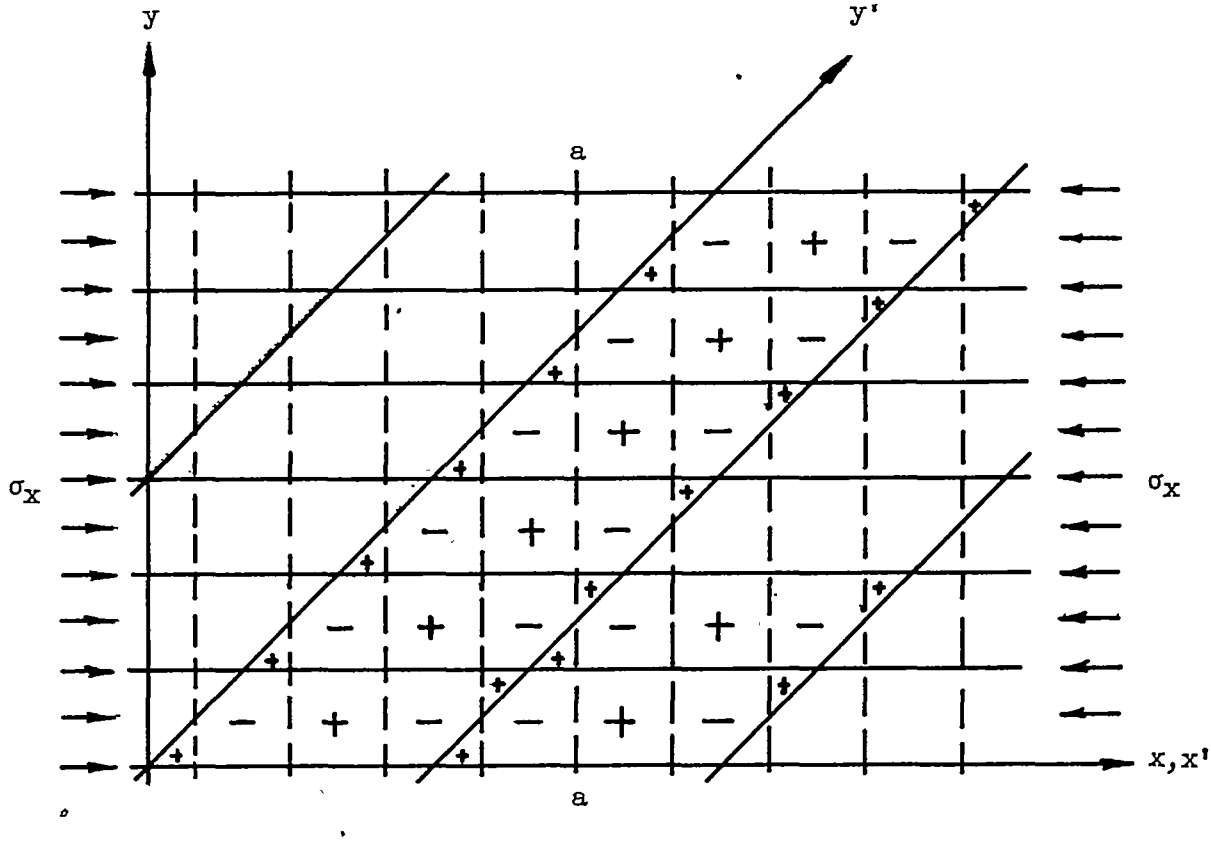

would be expected for compression in the x-direction whatever the skew angle or aspect ratio. Dashed lines, such as a-a, represent nodal lines.

In the sketch, the buckle pattern is represented as being symmetrical about a panel midpoint and repeating in every panel. However, in general, a repetitive buckle pattern can be assumed to take place in a group of panels of unknown dimensions Na in the x-direction and Nb' in the y'-direction, where N and M are integers.

A representation of such a pattern can be built up in two steps. First, zero deflection along all panel boundaries can be provided by the function

$$w_1 = \sin \frac{p\pi x'}{Na} \sin \frac{q\pi y'}{Mb'} \tag{A1}$$

where the ratios p/N and q/M are integers. For stress in the y-direction, equation (A1) with $\frac{p}{N} = 1$ and $\frac{q}{M} = 1, 2, 3, \ldots$ is a suitable approximation for the buckle pattern which occurs over a wide range of panel aspect ratio and skew angle ϕ. Similarly, the buckle pattern occurring in slightly skewed panels of moderate aspect ratio under stress in the x-direction is represented by equation (A1) with $\frac{p}{N} = 1, 2, 3, \ldots$ and $\frac{q}{M} = 1$. For this special case, the nodal lines a-a in the sketch are parallel to the y'-direction. In order to represent all other orientations of the nodal lines a-a and to permit an arbitrary uniform spacing, w_1 can be multiplied by some function such as w_2, where

$$w_2 = \cos \frac{j\pi}{Na}\left(x' \pm \frac{Na}{Mb'} y'\right) \tag{A2}$$

The lines along which $w_2 = 0$ have a slope determined by the ratio Na/Mb' and a spacing determined by the ratio j/N, where j is an integer and may take on all values 0, 1, 2, 3, ...

By multiplying w_1 by w_2, the desired deflection function

$$w = \sin \frac{p\pi x'}{Na} \sin \frac{q\pi y'}{Mb'} \cos \frac{j\pi}{Na}\left(x' \pm \frac{Na}{Mb'} y'\right) \tag{A3}$$

is obtained. This function is capable of satisfying the idealized physical characteristics of the buckle pattern for any panel aspect ratio and skew angle upon proper choice of the integers p, q, N, M, and j. Actually, it is necessary to consider only the plus sign in

equation (A3) under compression loading since the plus-sign case describes all natural orientations of nodal lines. Another form of equation (A3), more convenient for calculation purposes, is

$$w = \sin \frac{p\pi x'}{Na} \sin \frac{q\pi y'}{Mb'}\left(\cos \frac{j\pi x'}{Na} \cos \frac{j\pi y'}{Mb'} - \sin \frac{j\pi x'}{Na} \sin \frac{j\pi y'}{Mb'}\right) \quad (A4)$$

Energy expression.- The internal energy V of the plate and the external work T done by the loads, expressed in rectangular coordinates, are

$$V = \frac{D}{2}\int_0^{Na} \int_0^{Mb}\left[\left(\frac{\partial^2 w}{\partial x^2}\right)^2 + \left(\frac{\partial^2 w}{\partial y^2}\right)^2 + 2\mu \frac{\partial^2 w}{\partial x^2} \frac{\partial^2 w}{\partial y^2} + 2(1 - \mu)\left(\frac{\partial^2 w}{\partial x\, \partial y}\right)^2\right] dx\, dy \quad (A5)$$

and

$$T = \int_0^{Na} \int_0^{Mb} \left[\frac{\sigma_x t}{2}\left(\frac{\partial w}{\partial x}\right)^2 + \frac{\sigma_y t}{2}\left(\frac{\partial w}{\partial y}\right)^2\right] dx\, dy \quad (A6)$$

Conversion of the energy expression into the skew coordinate system (x',y') is accomplished with the transformation equations

$$x' = x - y \tan \phi$$

$$y' = \frac{y}{\cos \phi}$$

where the positive directions of the coordinates are shown in the following sketch:

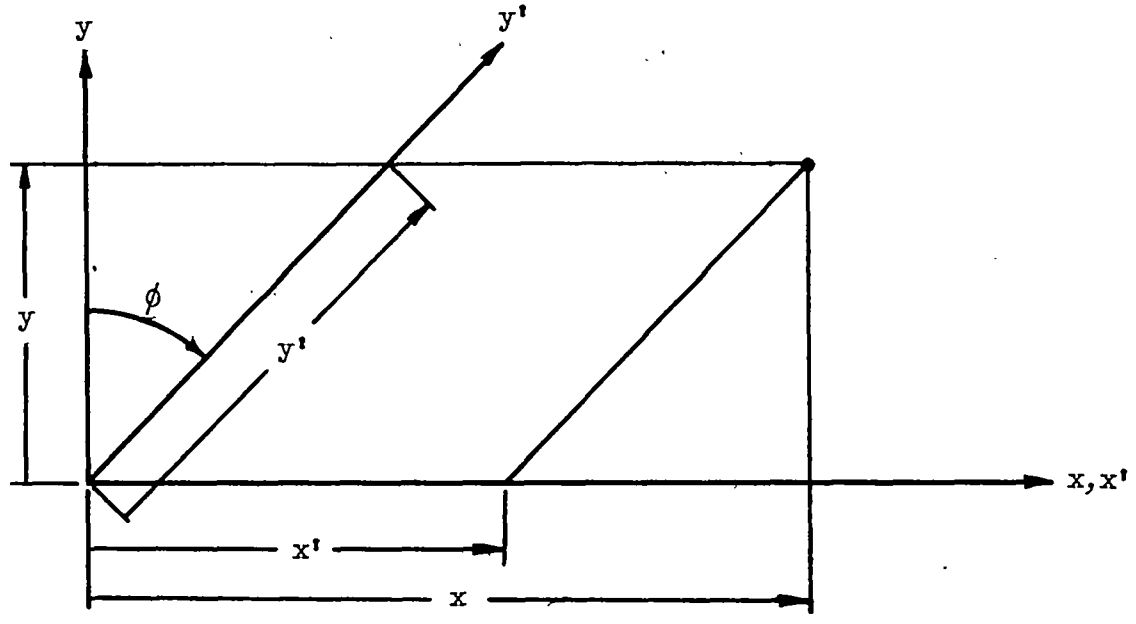

In the skew coordinate system, V and T become

$$V = \frac{D}{2\cos\phi}\int_0^{Na}\int_0^{Mb'}\left\{\frac{1}{\cos^2\phi}\left[\left(\frac{\partial^2 w}{\partial x'^2}\right)^2 + \left(\frac{\partial^2 w}{\partial y'^2}\right)^2\right] + \right.$$

$$\left[2(1-\mu) + 4\tan^2\phi\right]\left(\frac{\partial^2 w}{\partial x'\,\partial y'}\right)^2 + 2\left(\mu + \tan^2\phi\right)\frac{\partial^2 w}{\partial x'^2}\frac{\partial^2 w}{\partial y'^2} -$$

$$\left. 4\frac{\sin\phi}{\cos^2\phi}\frac{\partial^2 w}{\partial x'\,\partial y'}\left(\frac{\partial^2 w}{\partial x'^2} + \frac{\partial^2 w}{\partial y'^2}\right)\right\} dx\,dy \qquad \text{(A7)}$$

and

$$T = \int_0^{Na}\int_0^{Mb'}\left\{\frac{\sigma_x t\cos\phi}{2}\left(\frac{\partial w}{\partial x'}\right)^2 + \frac{\sigma_y t\cos\phi}{2}\left[\left(\frac{\partial w}{\partial x'}\right)^2\tan^2\phi - \right.\right.$$

$$\left.\left. 2\frac{\partial w}{\partial x'}\frac{\partial w}{\partial y'}\frac{\sin\phi}{\cos^2\phi} + \frac{1}{\cos^2\phi}\left(\frac{\partial w}{\partial y'}\right)^2\right]\right\} dx'\,dy' \qquad \text{(A8)}$$

As shown in equations (A7) and (A8), the integrations are performed over a repetitive buckle pattern.

Stability criteria.- By substituting equation (A4) for w into equations (A7) and (A8) and by setting V equal to T, the following stability criterion is obtained:

$$\frac{1}{\cos^2\phi}\left[\frac{1}{\beta'^2}\left(\frac{p^4}{N^4}+6\frac{p^2j^2}{N^4}+\frac{j^4}{N^4}\right)+\beta'^2\left(\frac{q^4}{M^4}+6\frac{q^2j^2}{M^4}+\frac{j^4}{M^4}\right)\right]+$$

$$2\left(\frac{p^2}{N^2}+\frac{j^2}{N^2}\right)\left(\frac{q^2}{M^2}+\frac{j^2}{M^2}\right)(1+3\tan^2\phi)-4\frac{j^2}{MN}\frac{\sin\phi}{\cos^2\phi}\left[\frac{1}{\beta'}\left(3\frac{p^2}{N^2}+\frac{j^2}{N^2}\right)+\right.$$

$$\left.\beta'\left(3\frac{q^2}{M^2}+\frac{j^2}{M^2}\right)\right]=k_x'\cos^2\phi\left(\frac{p^2}{N^2}+\frac{j^2}{N^2}\right)+k_y'\left[\left(\frac{p^2}{N^2}+\frac{j^2}{N^2}\right)\sin^2\phi-\right.$$

$$\left.2\beta'\frac{j^2}{MN}\sin\phi+\beta'^2\left(\frac{q^2}{M^2}+\frac{j^2}{M^2}\right)\right] \qquad (A9)$$

where

$$\beta' = \frac{a}{b'}$$

$$k_x' = \frac{\sigma_x t b'^2}{\pi^2 D}$$

and

$$k_y' = \frac{\sigma_y t b'^2}{\pi^2 D}$$

A somewhat more convenient form of equation (A9) for computational purposes is obtained if the skewed-plate aspect ratio is defined as a/b to conform with the usual notation for a rectangular plate of equal area. If the substitution $b' = \frac{b}{\cos \phi}$ is made, then $\frac{\beta'}{\cos \phi} = \beta$, $k_x' \cos^2\phi = k_x$, $k_y' \cos^2\phi = k_y$, and equation (A9) becomes

$$\frac{1}{\beta^2 \cos^4\phi}\left(\frac{p^4}{N^4} + 6\,\frac{p^2j^2}{N^4} + \frac{j^4}{N^4}\right) + \beta^2\left(\frac{q^4}{M^4} + 6\,\frac{q^2j^2}{M^4} + \frac{j^4}{M^4}\right) +$$

$$2\left(\frac{p^2}{N^2} + \frac{j^2}{N^2}\right)\left(\frac{q^2}{M^2} + \frac{j^2}{M^2}\right)\left(1 + 3\tan^2\phi\right) - 4\,\frac{j^2}{MN}\tan\phi\left[\frac{1}{\beta\cos^2\phi}\left(3\,\frac{p^2}{N^2} + \frac{j^2}{N^2}\right) +\right.$$

$$\left.\beta\left(3\,\frac{q^2}{M^2} + \frac{j^2}{M^2}\right)\right] = k_x\left(\frac{p^2}{N^2} + \frac{j^2}{N^2}\right) + k_y\left[\left(\frac{p^2}{N^2} + \frac{j^2}{N^2}\right)\tan^2\phi -\right.$$

$$\left.2\beta\,\frac{j^2}{MN}\tan\phi + \beta^2\left(\frac{q^2}{M^2} + \frac{j^2}{M^2}\right)\right] \qquad \text{(A10)}$$

The critical values of the buckling-stress coefficients k_x and k_y are determined by the values of the ratios p/N, j/N, q/M, j/M that make the coefficients a minimum.

If $\frac{j}{N} = \frac{j}{M} = 0$, which is equivalent to using equation (A1) for a deflection function, equation (A10) reduces to

$$\left(\frac{1}{\beta\cos^2\phi}\,\frac{p^2}{N^2} + \beta\,\frac{q^2}{M^2}\right)^2 + 4\tan^2\phi\,\frac{p^2q^2}{M^2N^2} = k_x\,\frac{p^2}{N^2} + k_y\left(\frac{p^2}{N^2}\tan^2\phi + \beta^2\,\frac{q^2}{M^2}\right) \qquad \text{(A11)}$$

This equation is the exact stability criterion for a rectangular plate in compression when ϕ is set equal to zero. The curves of buckling coefficient plotted against aspect ratio for stress in the y-direction in figure 4 were computed from equation (A11) by setting $k_x = 0$. Over

the range of aspect ratio covered, the lowest buckling coefficients were associated with the parameters $\frac{p}{N} = \frac{q}{M} = 1$, except for the part of the curve for $\phi = 0^\circ$ in the region $\frac{1}{\sqrt{6}} < \beta < \frac{1}{\sqrt{2}}$ for which the buckle pattern is defined by $\frac{p}{N} = 1$, $\frac{q}{M} = 2$.

For the special case $\beta = \frac{1}{\cos \phi}$, which specifies equal-sided panels, and for $\frac{p}{N} = \frac{q}{M} = 1$ and $k_x = 0$, equation (All) reduces to

$$4(1 + \sin^2\phi) = k_y(1 + \sin^2\phi)$$

or

$$k_y = 4$$

This result is the one obtained previously by substituting $w = \sin \frac{\pi x'}{a} \sin \frac{\pi y'}{a}$ into the plate differential equation.

A determination of the buckling-stress coefficients for stress in the x-direction from equation (A10) may be made when a buckle pattern has been specified by the parameters p/N, j/N, q/M, and j/M. For a given panel shape, several buckle patterns must be investigated to determine the pattern associated with the lowest buckling-stress coefficient. The minimum computed coefficients thus obtained are plotted in figure 2, and the parameters p/N, j/N, q/M, and j/M defining the buckle pattern in each part of these curves are tabulated in table 2. From the table, the data for $\phi = 45^\circ$ and $\beta = 3.2$ were used to sketch the buckle pattern shown in a previous section "Choice of deflection function." Similarly, the buckle pattern associated with any other panel configuration covered in figure 2 can be sketched by substituting the appropriate parameters from table 2 into the general deflection function, equation (A3). This procedure was followed in preparing figure 3.

The interaction curves in figure 5 were derived by trial-and-error solution of equation (A10) by the process explained in the previous paragraph. The parameters defining the buckle pattern in each segment of these curves are tabulated in table 3.

APPENDIX B

MORE ACCURATE SOLUTION FOR CRITICAL COMPRESSIVE STRESS OF FLAT PLATE CONTINUOUS OVER SKEWED SUPPORTS

The results obtained in appendix A serve as a useful guide in making a more accurate energy solution for the critical stresses because the basic characteristics of the mode of buckling for a number of skewed panel configurations have been determined. These data are given in tables 2 and 3. A study reveals that a number of the buckle patterns can be classified rather simply as being either symmetrical or antisymmetrical about the midpoint of each panel and repeating in each panel or over two panels. The solutions in this appendix are confined to these cases. Representation of such patterns is feasible with two-dimensional sine and cosine series and permits an energy solution for the critical stresses to an arbitrarily high degree of accuracy. The critical stresses thus obtained provide a check on the results in appendix A.

Deflection functions.- The trigonometric series representing the deflection were chosen to satisfy term by term the required conditions of zero deflection around the panel boundaries and continuity of slope between panels. The four buckling configurations investigated are as follows:

Symmetric buckling, periodic over a, b',

$$w = \sum_{m=2,4,6}^{\infty} \sum_{n=2,4,6}^{\infty} a_{mn} \sin \frac{m\pi x'}{a} \sin \frac{n\pi y'}{b'} +$$

$$\sum_{m=1,3,5}^{\infty} \sum_{n=1,3,5}^{\infty} b_{mn} \left[\cos \frac{(m-1)\pi x'}{a} - \cos \frac{(m+1)\pi x'}{a} \right] \left[\cos \frac{(n-1)\pi y'}{b'} - \cos \frac{(n+1)\pi y'}{b'} \right] \qquad \text{(B1a)}$$

Symmetric buckling, periodic over $2a$, $2b'$,

$$w = \sum_{m=1,3,5}^{\infty} \sum_{n=1,3,5}^{\infty} a_{mn} \sin \frac{m\pi x'}{a} \sin \frac{n\pi y'}{b'} + \sum_{m=2,4,6}^{\infty} \sum_{n=2,4,6}^{\infty} b_{mn} \left[\cos \frac{(m-1)\pi x'}{a} - \cos \frac{(m+1)\pi x'}{a} \right] \left[\cos \frac{(n-1)\pi y'}{b'} - \cos \frac{(n+1)\pi y'}{b'} \right] \tag{B1b}$$

Antisymmetric buckling, periodic over a, $2b'$,

$$w = \sum_{m=2,4,6}^{\infty} \sum_{n=1,3,5}^{\infty} a_{mn} \sin \frac{m\pi x'}{a} \sin \frac{n\pi y'}{b'} + \sum_{m=1,3,5}^{\infty} \sum_{n=2,4,6}^{\infty} b_{mn} \left[\cos \frac{(m-1)\pi x'}{a} - \cos \frac{(m+1)\pi x'}{a} \right] \left[\cos \frac{(n-1)\pi y'}{b'} - \cos \frac{(n+1)\pi y'}{b'} \right] \tag{B1c}$$

Antisymmetric buckling, periodic over $2a$, b',

$$w = \sum_{m=1,3,5}^{\infty} \sum_{n=2,4,6}^{\infty} a_{mn} \sin \frac{m\pi x'}{a} \sin \frac{n\pi y'}{b'} + \sum_{m=2,4,6}^{\infty} \sum_{n=1,3,5}^{\infty} b_{mn} \left[\cos \frac{(m-1)\pi x'}{a} - \cos \frac{(m+1)\pi x'}{a} \right] \left[\cos \frac{(n-1)\pi y'}{b'} - \cos \frac{(n+1)\pi y'}{b'} \right] \tag{B1d}$$

Substitution of these deflection functions into the energy expressions (equations (A7) and (A8)) and minimization of the potential-energy function (V - T) with respect to a_{mn} and b_{mn} leads to the desired stability equations.

Symmetric buckling, periodic over a, b'.- For symmetric buckling, periodic over a, b', the infinite set of stability equations derived from function (B1a) is

$$0 = a_{mn}A_{mn} + 4mn\left[b_{(m+1)(n+1)} - b_{(m+1)(n-1)} - b_{(m-1)(n+1)} + b_{(m-1)(n-1)}\right]\left(\frac{m^2}{\beta\cos^2\phi} + n^2\beta - \frac{\beta}{2}k_y\right)\tan\phi$$

$$(m = 2, 4, 6, \ldots)\ (n = 2, 4, 6, \ldots) \quad \text{(B2a)}$$

$$\begin{aligned}
0 = {} & b_{mn}B_{mn} + 4(m+1)(n+1)a_{(m+1)(n+1)}\left[\frac{(m+1)^2}{\beta\cos^2\phi} + \beta(n+1)^2 - \frac{\beta}{2}k_y\right]\tan\phi - 4(m+1)(n-1)a_{(m+1)(n-1)}\left[\frac{(m+1)^2}{\beta\cos^2\phi} + \beta(n-1)^2 - \frac{\beta}{2}k_y\right]\tan\phi - \\
& 4(m-1)(n+1)a_{(m-1)(n+1)}\left[\frac{(m-1)^2}{\beta\cos^2\phi} + \beta(n+1)^2 - \frac{\beta}{2}k_y\right]\tan\phi + 4(m-1)(n-1)a_{(m-1)(n-1)}\left[\frac{(m-1)^2}{\beta\cos^2\phi} + \beta(n-1)^2 - \frac{\beta}{2}k_y\right]\tan\phi - 2b_{m(n-2)}\left[\frac{m^4+6m^2+1}{\beta^2\cos^4\phi} + \right. \\
& \left. \beta^2(n-1)^4 + 2(1+3\tan^2\phi)(n-1)^2(m^2+1) - (k_x + k_y\tan^2\phi)(m^2+1) - \beta^2k_y(n-1)^2\right] - 2b_{m(n+2)}\left[\frac{m^4+6m^2+1}{\beta^2\cos^4\phi} + \beta^2(n+1)^4 + 2(1+3\tan^2\phi)(n+1)^2(m^2+1) - \right. \\
& \left. (k_x + k_y\tan^2\phi)(m^2+1) - \beta^2k_y(n+1)^2\right] - 2b_{(m-2)n}\left[\frac{(m-1)^4}{\beta^2\cos^4\phi} + \beta^2(n^4+6n^2+1) + 2(1+3\tan^2\phi)(m-1)^2(n^2+1) - (k_x + k_y\tan^2\phi)(m-1)^2 - \beta^2k_y(n^2+1)\right] - \\
& 2b_{(m+2)n}\left[\frac{(m+1)^4}{\beta^2\cos^4\phi} + \beta^2(n^4+6n^2+1) + 2(1+3\tan^2\phi)(m+1)^2(n^2+1) - (k_x + k_y\tan^2\phi)(m+1)^2 - \beta^2k_y(n^2+1)\right] + b_{(m-2)(n-2)}\left[\frac{(m-1)^4}{\beta^2\cos^4\phi} + \beta^2(n-1)^4 + \right. \\
& \left. 2(1+3\tan^2\phi)(m-1)^2(n-1)^2 - (k_x + k_y\tan^2\phi)(m-1)^2 - \beta^2k_y(n-1)^2\right] + b_{(m+2)(n+2)}\left[\frac{(m+1)^4}{\beta^2\cos^4\phi} + \beta^2(n+1)^4 + 2(1+3\tan^2\phi)(m+1)^2(n+1)^2 - \right. \\
& \left. (k_x + k_y\tan^2\phi)(m+1)^2 - \beta^2k_y(n+1)^2\right] + b_{(m-2)(n+2)}\left[\frac{(m-1)^4}{\beta^2\cos^4\phi} + \beta^2(n+1)^4 + 2(1+3\tan^2\phi)(m-1)^2(n+1)^2 - (k_x + k_y\tan^2\phi)(m-1)^2 - \beta^2k_y(n+1)^2\right] + \\
& b_{(m+2)(n-2)}\left[\frac{(m+1)^4}{\beta^2\cos^4\phi} + \beta^2(n-1)^4 + 2(1+3\tan^2\phi)(m+1)^2(n-1)^2 - (k_x + k_y\tan^2\phi)(m+1)^2 - \beta^2k_y(n-1)^2\right]
\end{aligned}$$

$$(m = 3, 5, 7, \ldots)(n = 3, 5, 7, \ldots) \quad \text{(B2b)}$$

$$0 = b_{1n}B_{1n} - 8(n-1)a_{2(n-1)}\left[\frac{4}{\beta\cos^2\phi} + \beta(n-1)^2 - \frac{\beta}{2}k_y\right]\tan\phi +$$

$$8(n+1)a_{2(n+1)}\left[\frac{4}{\beta\cos^2\phi} + \beta(n+1)^2 - \frac{\beta}{2}k_y\right]\tan\phi - b_{1(n+2)}\left[\frac{16}{\beta^2\cos^4\phi} +\right.$$

$$3\beta^2(n+1)^4 + 8(1+3\tan^2\phi)(n+1)^2 - 4(k_x + k_y\tan^2\phi) -$$

$$\left.3\beta^2k_y(n+1)^2\right] - b_{1(n-2)}\left[\frac{16}{\beta^2\cos^4\phi} + 3\beta^2(n-1)^4 +\right.$$

$$\left.8(1+3\tan^2\phi)(n-1)^2 - 4(k_x + k_y\tan^2\phi) - 3\beta^2k_y(n-1)^2\right] -$$

$$2b_{3n}\left[\frac{16}{\beta^2\cos^4\phi} + \beta^2(n^4 + 6n^2 + 1) + 8(1+3\tan^2\phi)(n^2+1) -\right.$$

$$\left.4(k_x + k_y\tan^2\phi) - \beta^2k_y(n^2+1)\right] + b_{3(n+2)}\left[\frac{16}{\beta^2\cos^4\phi} + \beta^2(n+1)^4 +\right.$$

$$\left.8(1+3\tan^2\phi)(n+1)^2 - 4(k_x + k_y\tan^2\phi) - \beta^2k_y(n+1)^2\right] +$$

$$b_{3(n-2)}\left[\frac{16}{\beta^2\cos^4\phi} + \beta^2(n-1)^4 + 8(1+3\tan^2\phi)(n-1)^2 -\right.$$

$$\left.4(k_x + k_y\tan^2\phi) - \beta^2k_y(n-1)^2\right]$$

$$(n = 3, 5, 7, \ldots) \quad \text{(B2c)}$$

$$0 = b_{m1}B_{m1} - 8(m-1)a_{(m-1)2}\left[\frac{(m-1)^2}{\beta\cos^2\phi} + 4\beta - \frac{\beta}{2}k_y\right]\tan\phi +$$

$$8(m+1)a_{(m+1)2}\left[\frac{(m+1)^2}{\beta\cos^2\phi} + 4\beta - \frac{\beta}{2}k_y\right]\tan\phi - b_{(m-2)1}\left[\frac{3(m-1)^4}{\beta^2\cos^4\phi} +\right.$$

$$\left.16\beta^2 + 8(1+3\tan^2\phi)(m-1)^2 - 3(k_x + k_y\tan^2\phi)(m-1)^2 - 4\beta^2k_y\right] -$$

$$b_{(m+2)1}\left[\frac{3(m+1)^4}{\beta^2\cos^4\phi} + 16\beta^2 + 8(1+3\tan^2\phi)(m+1)^2 -\right.$$

$$\left.3(k_x + k_y\tan^2\phi)(m+1)^2 - 4\beta^2k_y\right] - 2b_{m3}\left[\frac{m^4+6m^2+1}{\beta^2\cos^4\phi} + 16\beta^2 +\right.$$

$$\left.8(1+3\tan^2\phi)(m^2+1) - (k_x + k_y\tan^2\phi)(m^2+1) - 4\beta^2k_y\right] +$$

$$b_{(m+2)3}\left[\frac{(m+1)^4}{\beta^2\cos^4\phi} + 16\beta^2 + 8(1+3\tan^2\phi)(m+1)^2 -\right.$$

$$\left.(k_x + k_y\tan^2\phi)(m+1)^2 - 4\beta^2k_y\right] + b_{(m-2)3}\left[\frac{(m-1)^4}{\beta^2\cos^4\phi} + 16\beta^2 +\right.$$

$$\left.8(1+3\tan^2\phi)(m-1)^2 - (k_x + k_y\tan^2\phi)(m-1)^2 - 4\beta^2k_y\right]$$

$$(m = 3, 5, 7, \ldots) \quad \text{(B2d)}$$

$$0 = b_{11}B_{11} + 16a_{22}\left(\frac{4}{\beta\cos^2\phi} + 4\beta - \frac{\beta}{2}k_y\right)\tan\phi - 4b_{13}\left[\frac{4}{\beta^2\cos^4\phi} + 12\beta^2 + 8(1 + 3\tan^2\phi) - (k_x + k_y\tan^2\phi) - 3\beta^2k_y\right] - 4b_{31}\left[\frac{12}{\beta^2\cos^4\phi} + 4\beta^2 + 8(1 + 3\tan^2\phi) - 3(k_x + k_y\tan^2\phi) - \beta^2k_y\right] + 4b_{33}\left[\frac{4}{\beta^2\cos^4\phi} + 4\beta^2 + 8(1 + 3\tan^2\phi) - (k_x + k_y\tan^2\phi) - \beta^2k_y\right] \quad \text{(B2e)}$$

where

$$A_{mn} = \frac{m^4}{\beta^2\cos^4\phi} + n^4\beta^2 + 2m^2n^2(1 + 3\tan^2\phi) - m^2(k_x + k_y\tan^2\phi) - n^2\beta^2k_y$$

$$B_{mn} = \frac{4(m^4 + 6m^2 + 1)}{\beta^2\cos^4\phi} + 4\beta^2(n^4 + 6n^2 + 1) + 8(1 + 3\tan^2\phi)(m^2 + 1)(n^2 + 1) - 4(k_x + k_y\tan^2\phi)(m^2 + 1) - 4\beta^2k_y(n^2 + 1)$$

$$B_{1n} = \frac{32}{\beta^2\cos^4\phi} + 6\beta^2(n^4 + 6n^2 + 1) + 16(1 + 3\tan^2\phi)(n^2 + 1) - 8(k_x + k_y\tan^2\phi) - 6\beta^2k_y(n^2 + 1)$$

$$B_{m1} = \frac{6(m^4 + 6m^2 + 1)}{\beta^2 \cos^4\phi} + 32\beta^2 + 16(1 + 3\tan^2\phi)(m^2 + 1) -$$

$$6(k_x + k_y \tan^2\phi)(m^2 + 1) - 8\beta^2 k_y$$

$$B_{11} = \frac{48}{\beta^2 \cos^4\phi} + 48\beta^2 + 32(1 + 3\tan^2\phi) - 12(k_x + k_y \tan^2\phi) - 12\beta^2 k_y$$

The stability criterion is obtained by equating to zero the determinant formed by the coefficients of a_{mn} and b_{mn} in equations (B2). The numerical results calculated from this set of equations may be found in table 1. In each case four of each of the coefficients a_{mn} and b_{mn}, which gave an eighth-order determinant, were used in the calculations to insure an adequate representation of the buckle pattern.

Symmetric buckling, periodic over 2a, 2b'.- For symmetric buckling, periodic over 2a and 2b', the infinite set of stability equations derived from the function (B1b) is the same as that derived from the function (B1a) except for a change in the values of m and n involved. For the buckle pattern now under consideration, equations (B2a) exist for $m = 1, 3, 5, \ldots$ and $n = 1, 3, 5, \ldots$. Similarly, equations (B2b) exist for $m = 2, 4, \ldots$ and $n = 2, 4, \ldots$, and equations (B2c), (B2d), and (B2e) do not exist. Note should be taken that coefficients with the subscripts $m - 1$ and $n - 1$ in equations (B2a) drop out for $m = n = 1$ since coefficients with a zero subscript do not appear in the deflection function (B1b). For the same reason coefficients with the subscripts $m - 2$ and $n - 2$ should be dropped from equations (B2b) for $m = n = 2$.

The numerical results calculated for certain panel configurations, in which a symmetrical buckle pattern repeating over 2a and 2b' is associated with the lowest buckling load, are given in table 1. For the panels in which $\phi = 30^\circ$ and 45°, four equations involving a_{11}, a_{13}, a_{31}, and b_{22} were employed in the calculations. For the panels of 60° skew, four of each of the coefficients a_{mn} and b_{mn} were required to provide an adequate representation of the buckle pattern.

Antisymmetric buckling, periodic over a, 2b'.- For antisymmetric buckling, periodic over a and 2b', the infinite set of stability equations derived from the function (B1c) may be written directly from

equations (B2a) to (B2c). For this buckle pattern, equations (B2a) exist for $m = 2, 4, 6, \ldots$ and $n = 1, 3, 5, \ldots$; equations (B2b) exist for $m = 3, 5, 7, \ldots$ and $n = 2, 4, 6, \ldots$; equations (B2c) exist for $n = 2, 4, 6, \ldots$; and equations (B2d) and (B2e) do not exist. The buckling coefficient k_x for loading in the x-direction was calculated for the panel configuration $\phi = 60^\circ$, $\beta = 3$ for which this buckle pattern applies, and a value $k_x = 6.95$ was obtained. This result was obtained when four a's and four b's were used in the deflection series (B1c).

Antisymmetric buckling, periodic over 2a, b'.- For antisymmetric buckling, periodic over 2a and b', the infinite set of stability equations derived from the function (B1d) may be written directly from equations (B2a) to (B2d). For this buckle pattern, equations (B2a) exist for $m = 1, 3, 5, \ldots$ and $n = 2, 4, 6, \ldots$; equations (B2b) exist for $m = 2, 4, 6, \ldots$ and $n = 3, 5, 7, \ldots$; equations (B2c) do not exist; equations (B2d) exist for $m = 2, 4, 6, \ldots$; and equation (B2e) does not exist.

Calculations were carried out for $\phi = 60^\circ$, $\beta = 1.2$, a panel configuration for which this buckle pattern applies. An adequate representation of the deflection was obtained when four a's and four b's were used in the deflection series (B1d) which gave a value of $k_x = 16.22$.

As was pointed out in the beginning of this appendix, these more accurate solutions were carried out only for those panels for which the mode of buckling was relatively simple and clearly indicated by the results of appendix A. In the absence of such information it would be necessary to investigate all conceivable modes of buckling for a given panel configuration.

REFERENCES

1. Timoshenko, S.: Theory of Elastic Stability. McGraw-Hill Book Co., Inc., 1936, p. 382.

2. Salvadori, Mario G.: Numerical Computation of Buckling Loads by Finite Differences. Proc. A.S.C.E., vol. 75, no. 10, Dec. 1949, p. 1471.

3. Budiansky, Bernard, Connor, Robert W., and Stein, Manuel: Buckling in Shear of Continuous Flat Plates. NACA TN 1565, 1948.

TABLE 1.- CRITICAL COMBINATIONS OF σ_x AND σ_y TYPES OF STRESS ACTING ON CONTINUOUS FLAT SHEET DIVIDED INTO PARALLELOGRAM-SHAPED PANELS

(DATA FOR CIRCLES IN FIGS. 2 TO 5)

$$\left[\sigma_x t = \frac{k_x \pi^2 D}{b^2};\ \sigma_y t = \frac{k_y \pi^2 D}{b^2}\right]$$

β	Stress combination		Buckle pattern		
	k_x	k_y	Symmetry (1)	Periodicity	
$\phi = 30°$					
0.5	0	19.33	S	2a	2b'
.577	9.60	0	S	2a	2b'
1.0	6.74	0	S	2a	2b'
1.155	6.62	0	S	2a	2b'
1.155	0	4	S	2a	2b'
3.0	0	1.41	S	2a	2b'
$\phi = 45°$					
0.5	24.12	0	S	2a	2b'
.6	0	14.32	S	2a	2b'
1.0	0	6.499	S	2a	2b'
1.0	11.46	0	S	a	b'
1.414	0	4	S	2a	2b'
1.414	5.99	2	S	2a	2b'
1.414	7.46	1	S	a	b'
2.0	6.36	0	A-S	2a	b'
3.0	5.11	0	S	a	b'
3.0	0	1.74	S	2a	2b'
$\phi = 60°$					
0.6	0	19.28	S	2a	2b'
1.0	0	9.25	S	2a	2b'
1.2	16.22	0	A-S	2a	b'
1.6	12.32	0	S	a	b'
2.0	0	4	S	2a	2b'
2.0	4.0	3.43	S	2a	2b'
2.0	7.14	2	S	2a	2b'
2.0	7.97	1	S	a	b'
2.0	8.75	0	S	a	b'
3.0	6.95	0	A-S	a	2b'
3.0	0	2.56	S	2a	2b'

[1] S - symmetrical about panel midpoint
A-S - antisymmetrical about panel midpoint.

TABLE 2.- DATA DEFINING THE BUCKLING MODES IN FIGURES 2 AND 3

[General modal function $w = \sin \frac{p\pi x'}{Na} \sin \frac{q\pi y'}{Mb'} \cos \frac{j\pi}{Na}\left(x' + \frac{Na}{Mb'} y'\right)$]

β	p/N	q/M	j/N	j/M	p/N	q/M	j/N	j/M	p/N	q/M	j/N	j/M
	$\phi = 0°$				$\phi = 15°$				$\phi = 30°$			
1.0	1	1	0	0	1	1	0	0	1	1	0	0
1.6	2	1	0	0	2	1	0	0	1	1	1	1/2
2.55	3	1	0	0	3	1	0	0	1	1	2	1/2
3.0	3	1	0	0	1	1	3	1/4	1	1	3	3/5
3.8	4	1	0	0	1	1	4	1/3	1	1	4	4/7
4.2	4	1	0	0	1	1	4	1/4	1	1	4	4/7
	$\phi = 45°$				$\phi = 60°$							
0.6	1	1	0	0	1	1	1	3				
.9	1	1	2/3	1	1	1	2	4				
1.2	1	1	1	1	1	1	2	3				
1.4	1	1	3/2	1	1	1	2	3				
1.8	1	1	2	4/3	1	1	3	3				
2.1	1	1	2	1	1	1	3	3				
2.5	1	1	5/2	1	1	1	3	2				
3.2	1	1	3	1	1	1	4	2				
4.2	1	1	4	1	1	1	5	2				

TABLE 3.- DATA DEFINING THE BUCKLING MODES IN FIGURE 5

k_x	p/N	q/M	j/N	j/M
$\phi = 0°, 30°$				
4	1	1	0	0
5	1	1	0	0
6	1	1	0	0
$\phi = 45°$				
4	1	1	0	0
5	1	1	0	0
6	1	1	0	0
7	1	1	1	1
8.5	1	1	3/2	1
$\phi = 60°$				
4	1	1	0	0
5	1	1	1	1
6	1	1	3/2	3/2
7	1	1	2	2
8.5	1	1	3	3

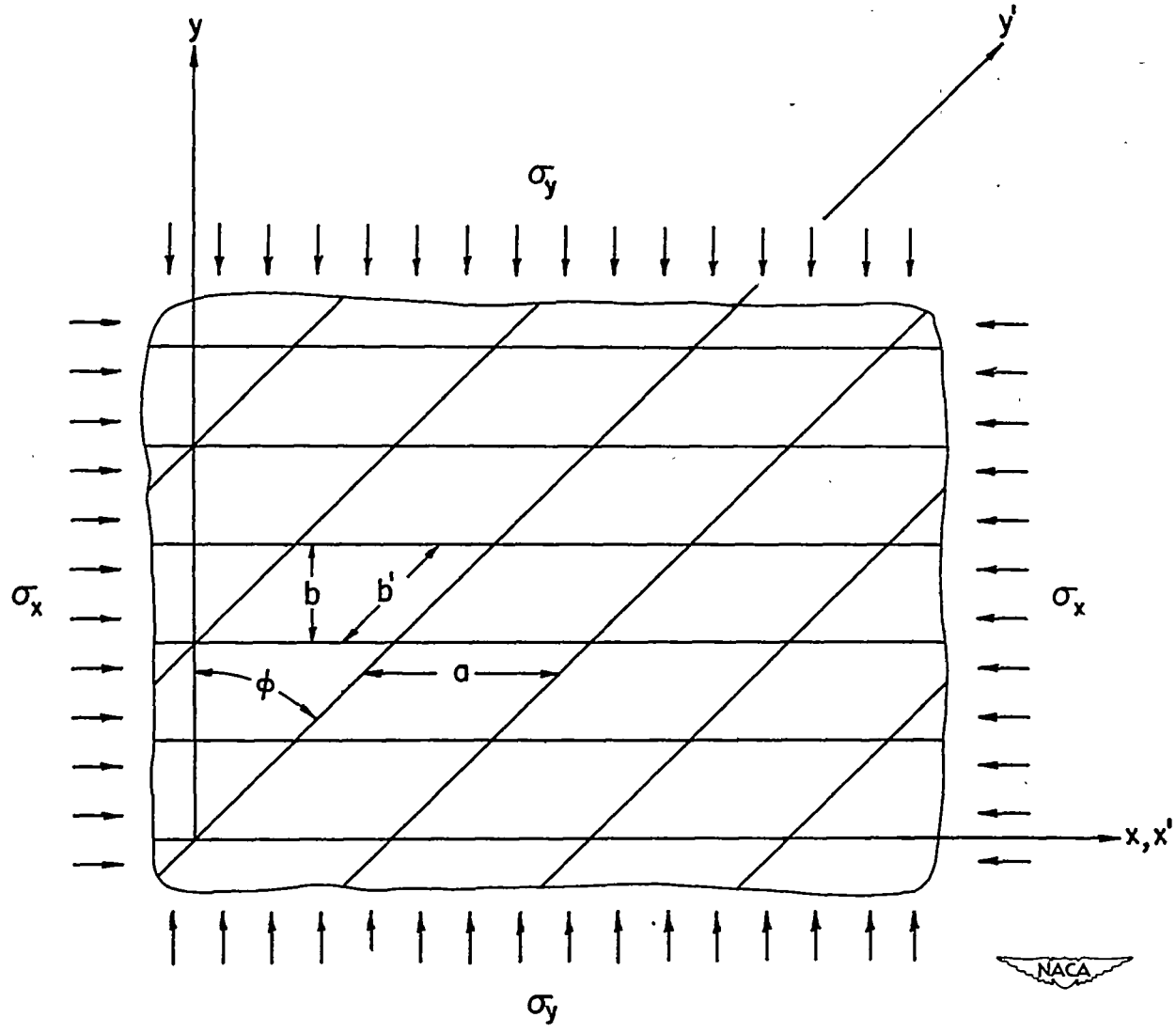

Figure 1.- Part of continuous flat sheet divided into parallelogram-shaped panels by nondeflecting supports.

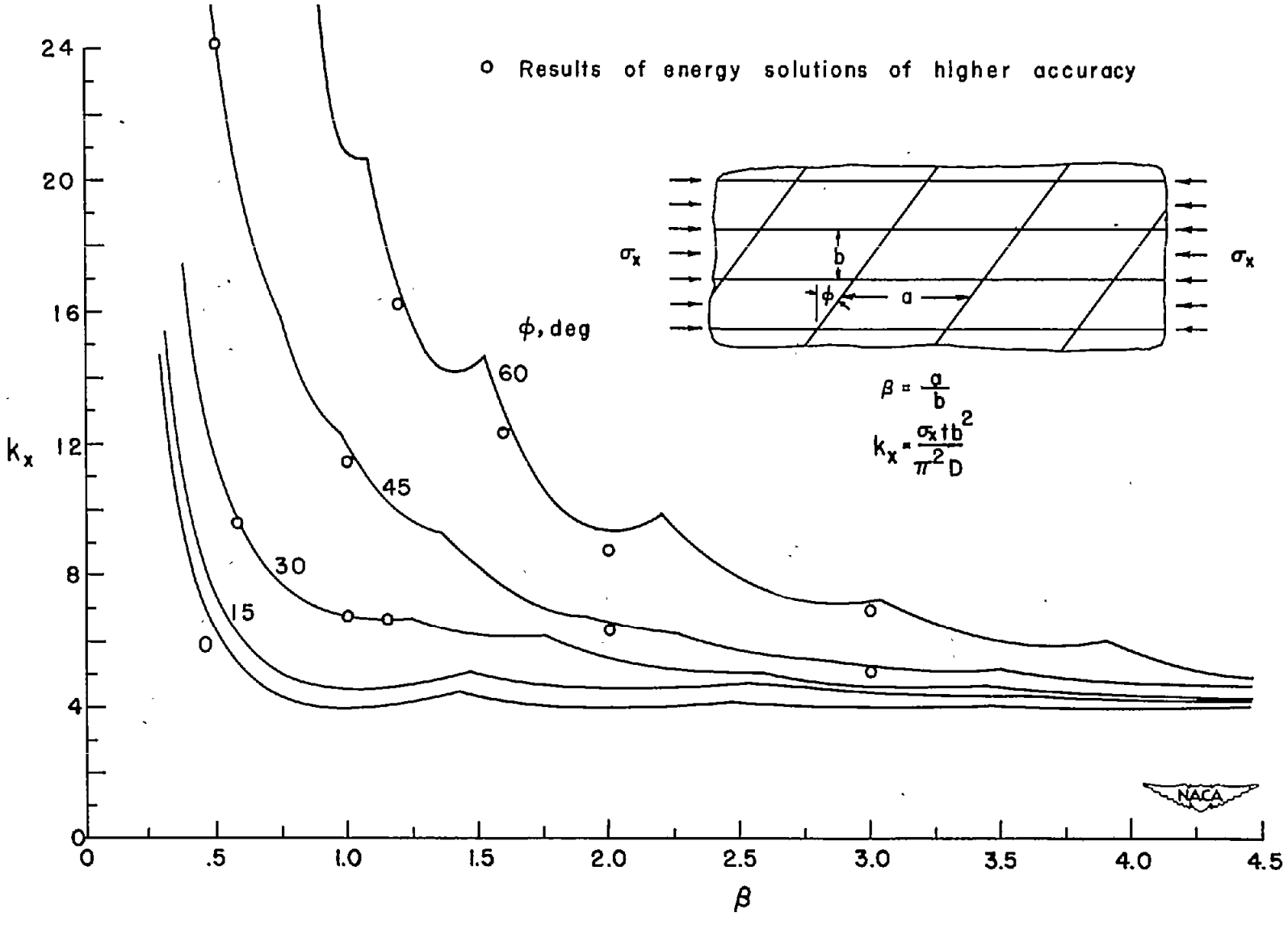

Figure 2.- Theoretical buckling stresses for parallelogram-shaped panels for stress acting parallel to a set of sides.

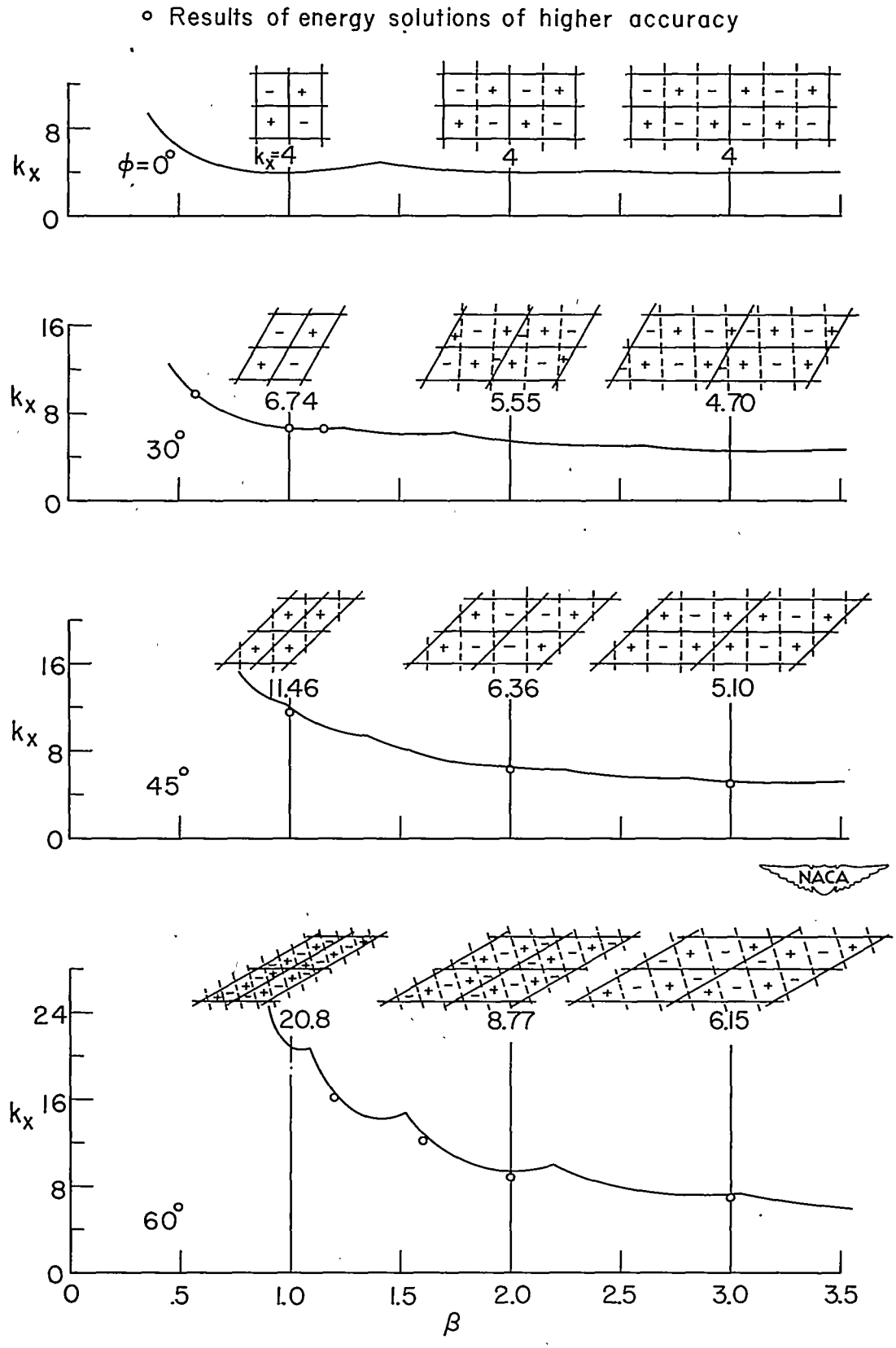

Figure 3.- Illustration of the variation in panel stability with changes in panel geometry. (Idealization of buckling mode shown in each panel.)

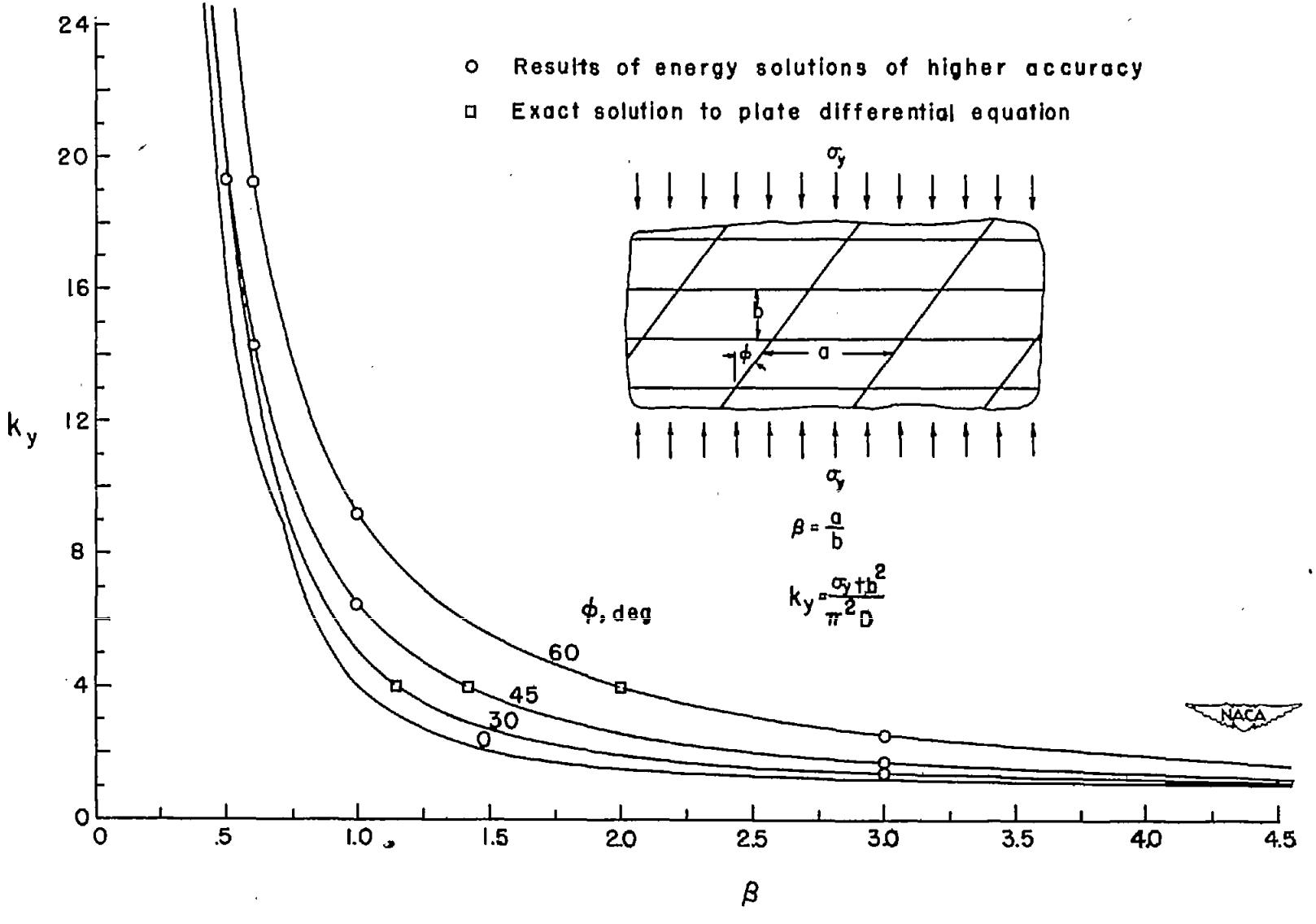

Figure 4.- Theoretical buckling stresses for parallelogram-shaped panels for stress acting perpendicular to a set of sides.

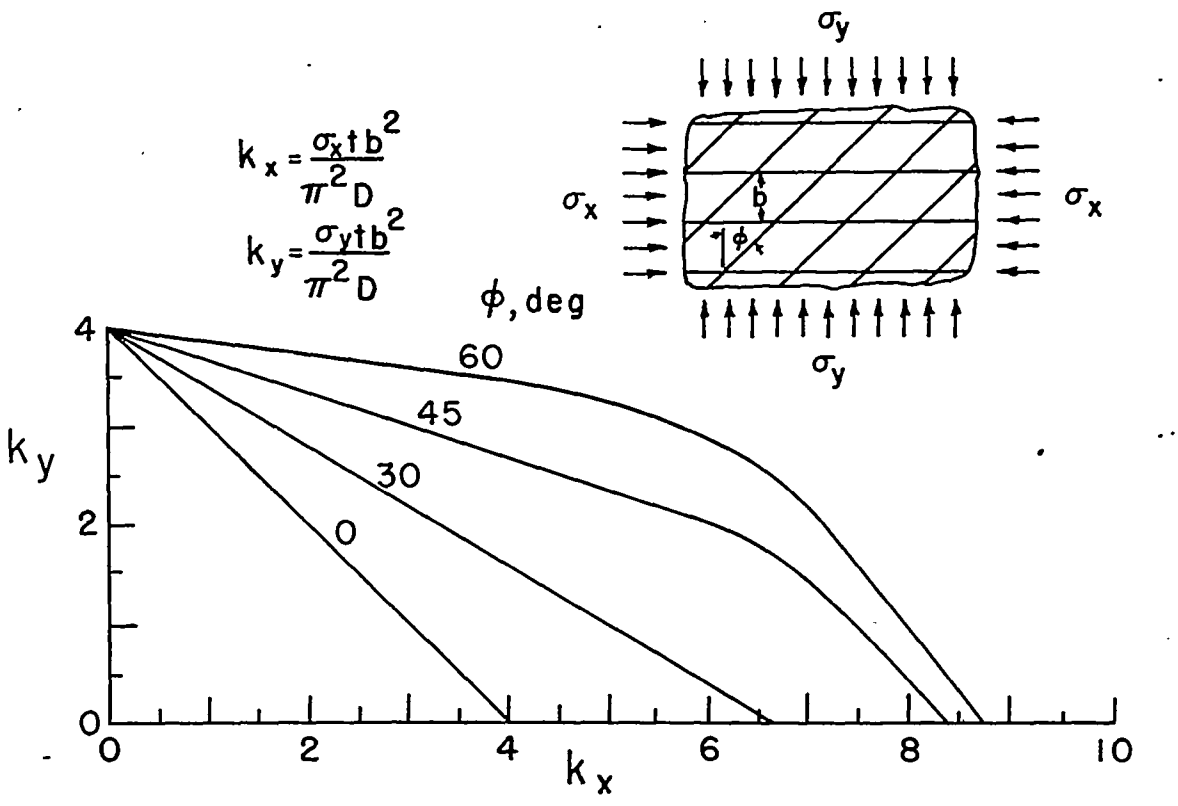

(a) Adjusted interaction curves.

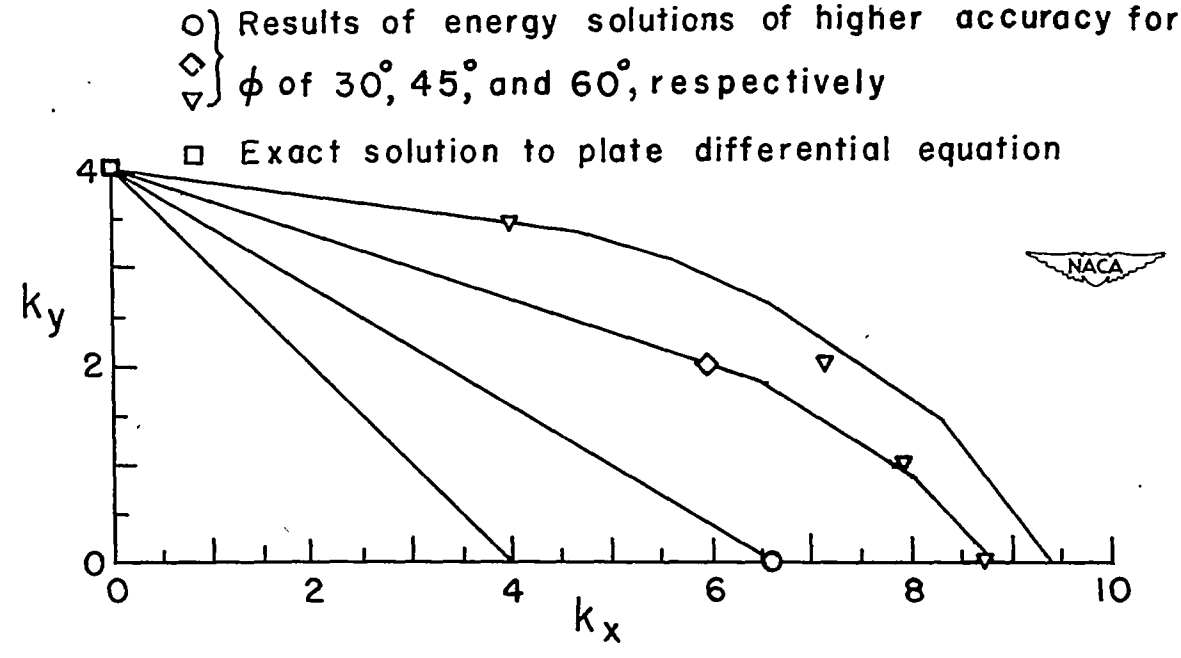

(b) Comparison of various solutions.

Figure 5.- Stability of equal-sided skew panels under simultaneous action of stresses in x- and y-directions.

NACA-Langley - 7-2-51 - 1000